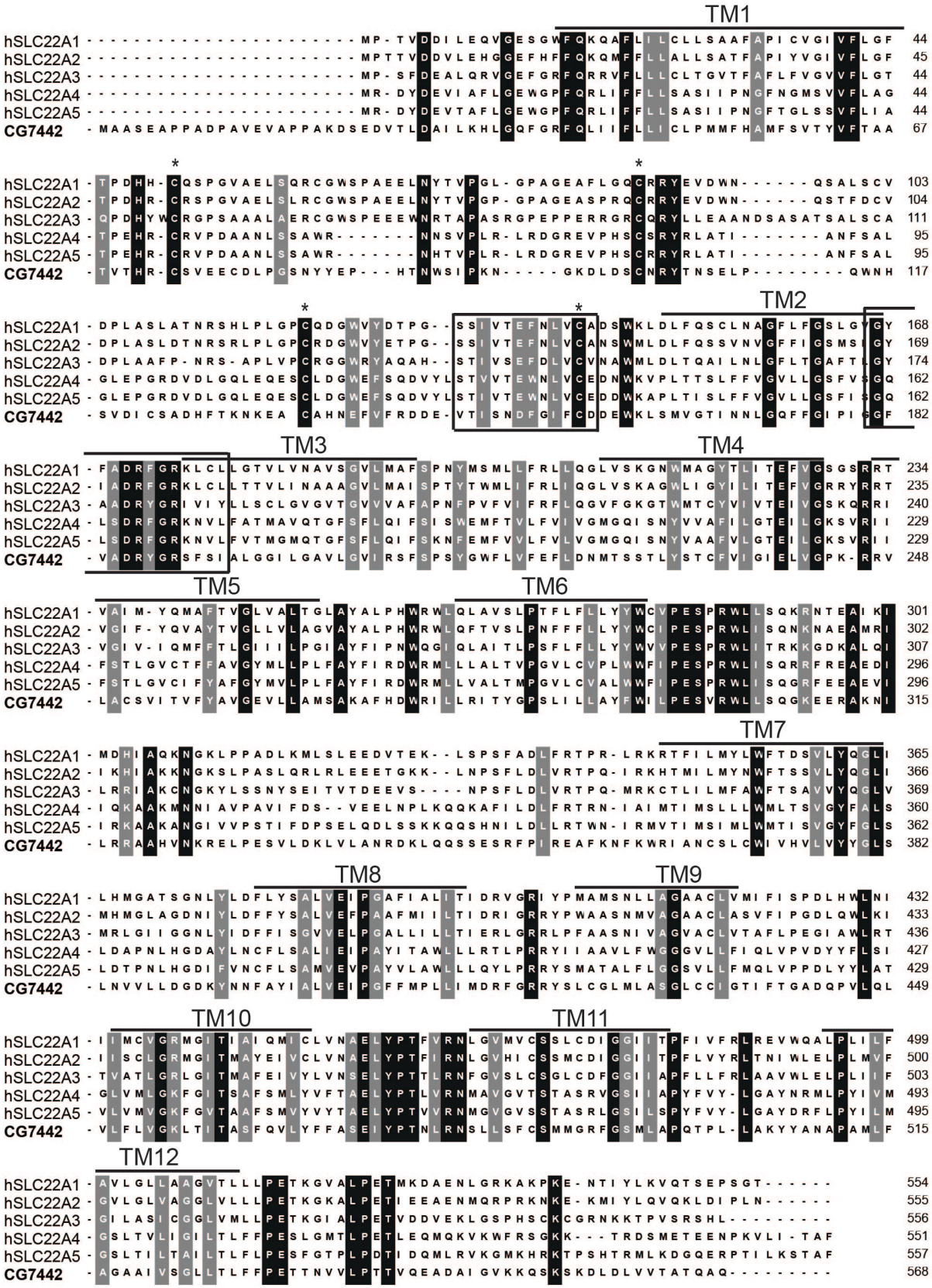
TM1
TM2
TM3
TM4
TM5
TM6
TM7
TM8
TM9
TM10
TM11
TM12
hSLC22A1
hSLC22A2
hSLC22A3
hSLC22A4
hSLC22A5
CG7442

Figure S1, Related to Figure 1. Sequence homology between CG7442, other related *Drosophila* genes, and members of the human SLC22A family. Sequence alignment of *Drosophila* CG7442 and human SLC22 family members A1-A5. Predicted transmembrane domains (TDs) are overlined. Amino acids identities are highlighted in black; gray shading highlights amino acid similarity. The ASF (amphiphilic solute facilitator) and MSF (major facilitator superfamily) signature motifs for the family are boxed. Asterisks (*) mark four cysteine residues with potential functional conservation in the extracellular loop.

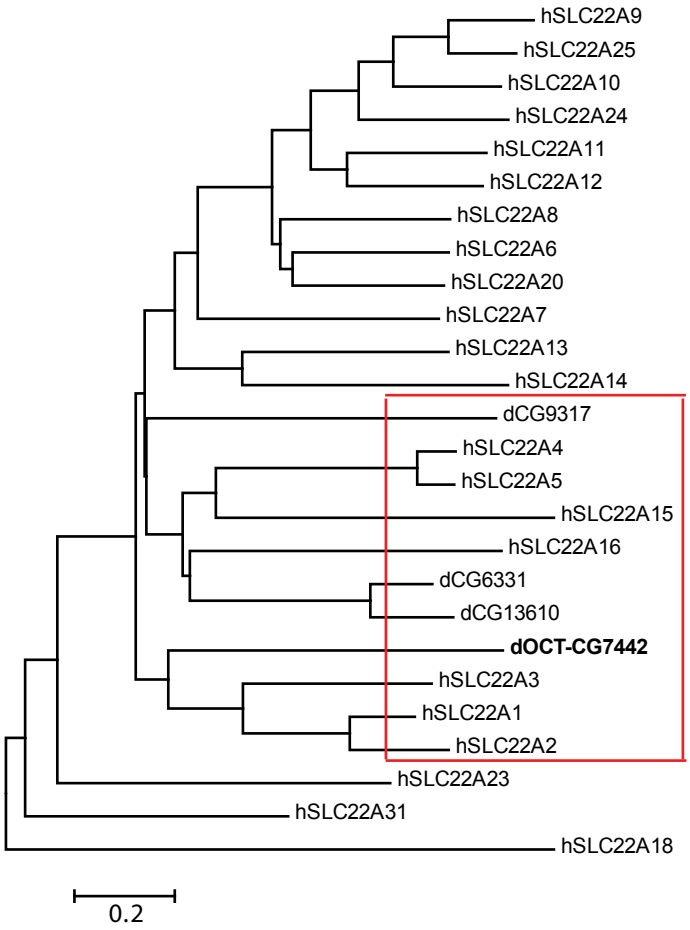
hSLC22A9
hSLC22A25
hSLC22A10
hSLC22A24
hSLC22A11
hSLC22A12
hSLC22A8
hSLC22A6
hSLC22A20
hSLC22A7
hSLC22A13
hSLC22A14
dCG9317
hSLC22A4
hSLC22A5
hSLC22A15
hSLC22A16
dCG6331
dCG13610
dOCT-CG7442
hSLC22A3
hSLC22A1
hSLC22A2
hSLC22A23
hSLC22A31
hSLC22A18
0.2

Figure S2, Related to Figure 1. Dendrogram of human and *Drosophila* SLC22A family members with *Drosophila* CG7442. There are four members in *Drosophila* of the SLC22A family (CG9317, CG6331, CG13610, CG7442). CG7442 is more related to organic cation transporters (hSLC22A1-5, 15 and 16) (boxed) than organic anion transporters (hSLC22A6-14, 20). The scale bar represents 0.2 molecular operational taxonomic units.

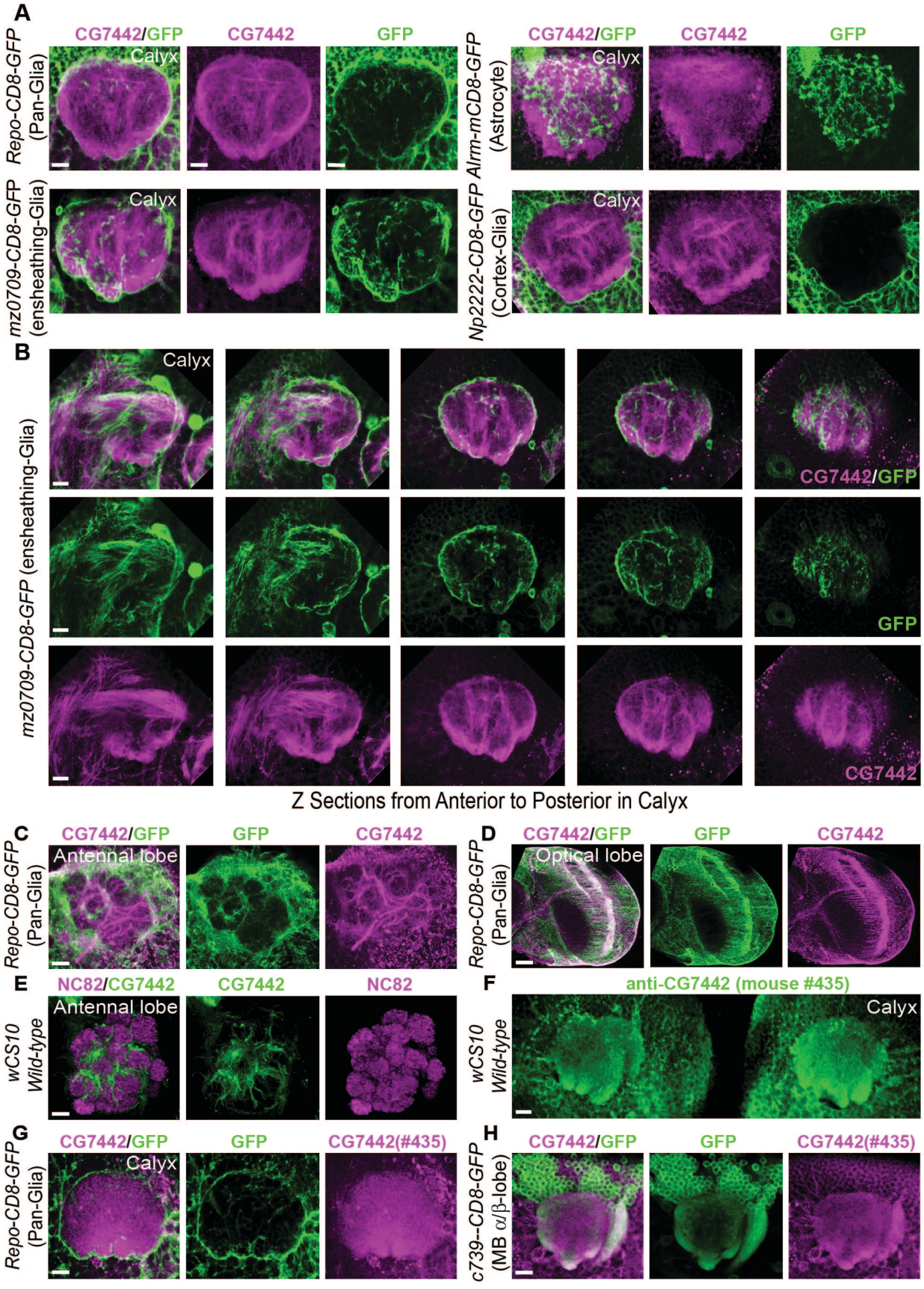
A
CG7442/GFP
CG7442
GFP
Repo-CD8-GFP (Pan-Glia)
Calyx
Alrm-mCD8-GFP (Astrocyte)
mz0709-CD8-GFP (ensheathing-Glia)
Np2222-CD8-GFP (Cortex-Glia)
B
mz0709-CD8-GFP (ensheathing-Glia)
Z Sections from Anterior to Posterior in Calyx
C
Antennal lobe
D
Optical lobe
E
NC82/CG7442
NC82
wCS10 Wild-type
F
anti-CG7442 (mouse #435)
G
CG7442(#435)
H
c739--CD8-GFP (MB α/β-lobe)

Figure S3, Related to Figure 3. DmSLC22A expression does not overlap with glial markers.

(A) Images of the calyx for expression of a UAS-GFP reporter transgene in all glia cells using *Repo-gal4*, in astrocytes with *Alrm-gal4*, in ensheathing glia with *mz0709-gal4*, and in cortex-glia with *Np2222-gal4*. The anti-DmSLC22A signal is shown in magenta. There was no large co-localization of the two signals in the MB calyx. **(B)** Expression of UAS-GFP reporter transgene in ensheathing glia by *mz0709-gal4* near the calyx. Anti-DmSLC22A expression is shown in magenta. This shows a series of frontal Z-sections at the level of the calyx from anterior to posterior. **(C-D)** Marking glial structures and anti-DmSLC22A immunoreactivity in the antennal and optic lobes. There was no obvious overlap of expression in the antennal lobe. Some overlap in expression was observed in the optic lobe in the form of a crescent shaped structure. (**E**) Double-labeling with anti-DmSLC22A (green) and the presynaptic marker anti-Brp^{nc82} (magenta) in antennal lobe showed no co-localization of two signals. (**F-H**) Images of the MB calyx decorated by mouse monoclonal anti-DmSLC22A, a second antibody made to the protein. This further confirmed the dendritic accumulation of DmSLC22A at the calyx, which largely overlaps with the α/β MBn-specific GFP signals, but shows no obvious overlap with glial GFP signals driven by *Repo-gal4.* DmSLC22A distribution is shown in green in panel **F**, and in magenta in panel **G-H**. Scale bars = 10 μm.

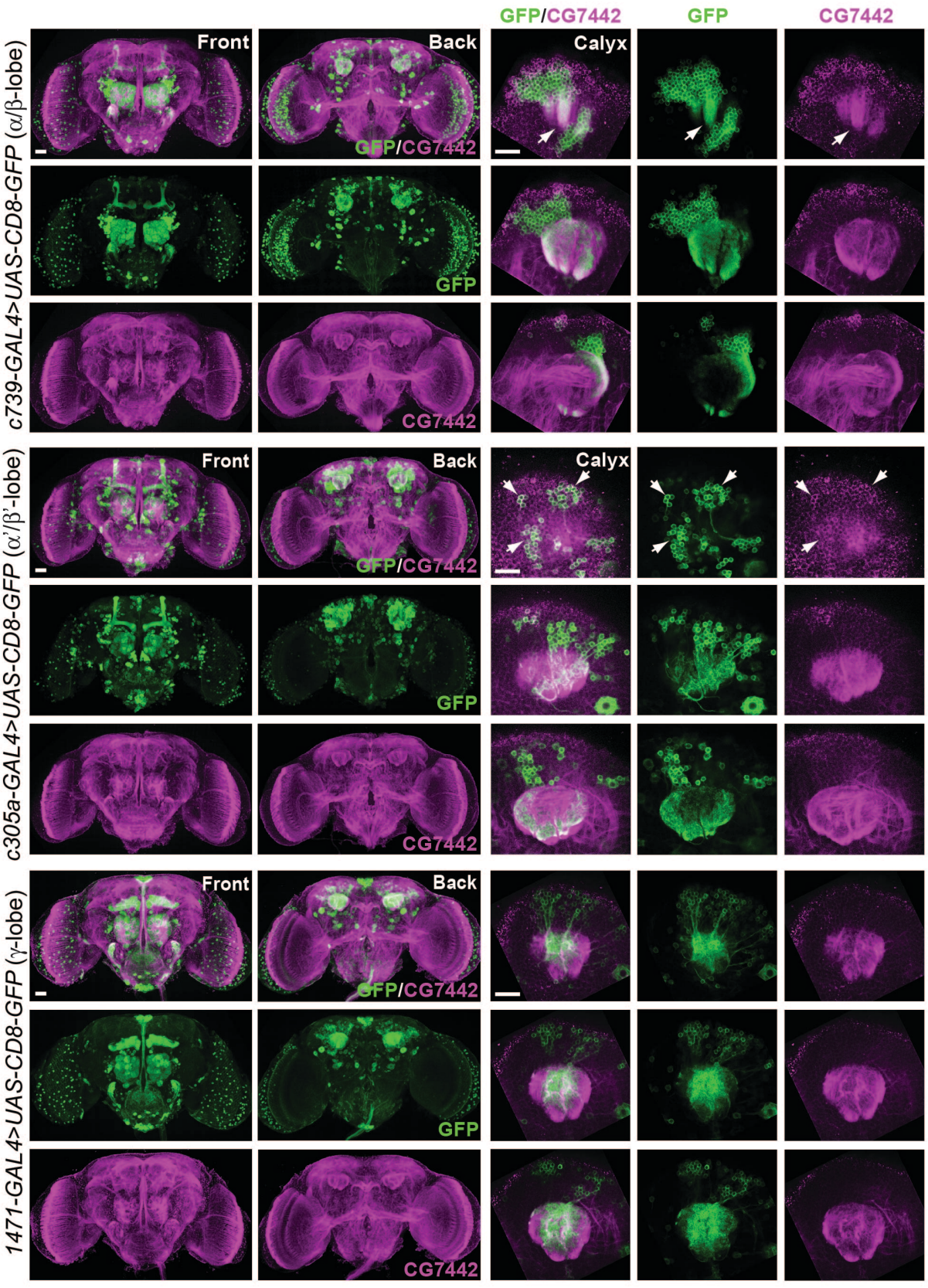
GFP/CG7442
GFP
CG7442
Front
Back
Calyx
GFP/CG7442
GFP
CG7442
c739-GAL4>UAS-CD8-GFP (α/β-lobe)
Front
Back
Calyx
GFP/CG7442
GFP
CG7442
c305a-GAL4>UAS-CD8-GFP (α'/β'-lobe)
Front
Back
GFP/CG7442
GFP
CG7442
1471-GAL4>UAS-CD8-GFP (γ-lobe)

Figure S4, Related to Figure 3. DmSLC22A expression in α/β and α'/β' MBn.
GFP reporter expression in the α/β neurons (*c739-gal4)*, α'/β' neurons (*c305a-gal4)* and γ neurons (*1471-gal4)* is shown in green, and anti-DmSLC22A in magenta. The left two columns depict low-resolution images from the front and the back of the brain. The right three columns depict high-resolution images of the calyx, with each row representing a 1.5 µm sub-stack at a different position along the anterior/posterior axis. There is strong overlap in signals in the α/β neurons, notably, in three, broad vertical stripes in the anterior calyx (arrows). The DmSLC22A immunoreactivity is primarily in the neuropil; the cell body staining is relatively weak. Overlap of signals in the α'/β' neurons is most obvious in the cell bodies, with a possible overlap of signal as a diagonal stripe within the calyx (arrow). A slight overlap in expression can be discerned in the γ neurons, although some of that shown here is not observed in single confocal slices. Scale bar = 20 µm.

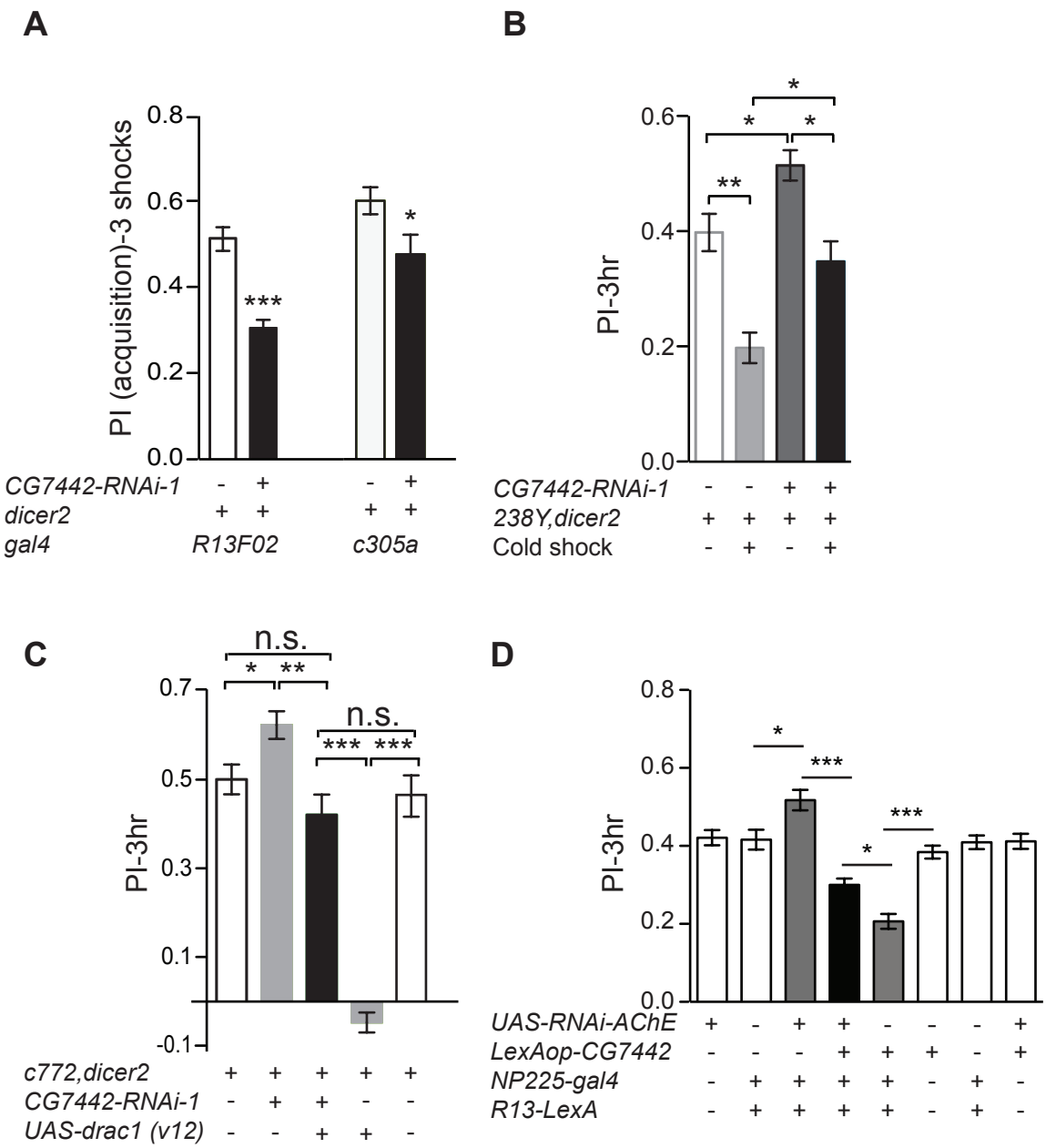
A
PI (acquisition)-3 shocks
0.8
0.6
0.4
0.2
0.0
***
*
CG7442-RNAi-1 - + - +
dicer2 + + + +
gal4 R13F02 c305a
B
PI-3hr
0.6
0.4
0.2
0.0
*
*
*
**
CG7442-RNAi-1 - - + +
238Y,dicer2 + + + +
Cold shock - + - +
C
PI-3hr
0.7
0.5
0.3
0.1
-0.1
n.s.
*
**
n.s.
***
***
c772,dicer2 + + + + +
CG7442-RNAi-1 - + + - -
UAS-drac1 (v12) - - + + -
D
PI-3hr
0.8
0.6
0.4
0.2
0.0
*
***
***
*
UAS-RNAi-AChE + - + + - - - +
LexAop-CG7442 - - - + + + - +
NP225-gal4 - + + + + - + -
R13-LexA - + + + + - + -

Figure S5, Related to Figure 5 and 8. DmSLC22A is functionally required in the MBn for memory.

(A) Memory acquisition using 3-shock conditioning. Flies expressing *CG7442-RNAi-1* in all MBn (*R13F02-gal4*) or α'/β' MBn (*c305-gal4*) were impaired in performance compared to the control genotype using 3 shock training (see Figure 5C)**. (B)** Cold-shock induced anesthesia was performed at 1.5h after conditioning and 3h memory measured. Flies with the DmSLC22A knockdown showed enhanced cold-shock resistant and sensitive memory components. *Statistics:* One-way ANOVA and Tukey's post hoc comparisons with **P*<0.05, ***P*<0.01. N=6-8 for each group. **(C)** Lack of genetic interaction between *drac1* and *CG7442*. When the *CG7442-RNAi-1* transgene was combined with a constitutively active *drac1* transgene and driven with a MBn driver, *c772-gal4*, the memory performance was intermediate between that of the two parental flies and more similar to control genotypes. This shows that neither of the two parental phenotypes was epistatic to the other, suggesting that DmSLC22A suppresses memory in a pathway independent of the Rac-defined forgetting pathway. *Statistics:* One-way ANOVA and Tukey's post hoc comparisons with **P*<0.05, ***P*<0.01, ****P*<0.001. N=6-8 for each group**. (D)** Genetic manipulation of cholinergic neurotransmission at Pn:MBn synapses. Reducing AChE with RNAi expression in the Pn (*NP225-gal4)* enhanced memory expression, while overexpression of DmSLC22A in the MBn (*R13-LexA)* impaired memory expression. Overexpression of DmSLC22A in the MBn suppressed the enhanced memory expression due to AChE knockdown in the Pn. The genotypes of for the 2nd and 7th bars are *NP225-gal4;R13-LexA*>60100 and *NP225-gal4;R13-LexA*>8622, respectively. The 8622 line harbors the *P{CaryP}attP2* site, the docking site for the *LexAop* transgene. The former genotype serves as the control for RNAi expression; the latter as the control for *LexAop-DmSLC22A* expression. *Statistics:* Results are plotted as means ± SEM with * *P*<0.05, ** *P*<0.01, *** *P*<0.001. One-way ANOVA with Tukey's *post hoc* comparisons. N=11-12 for all groups.

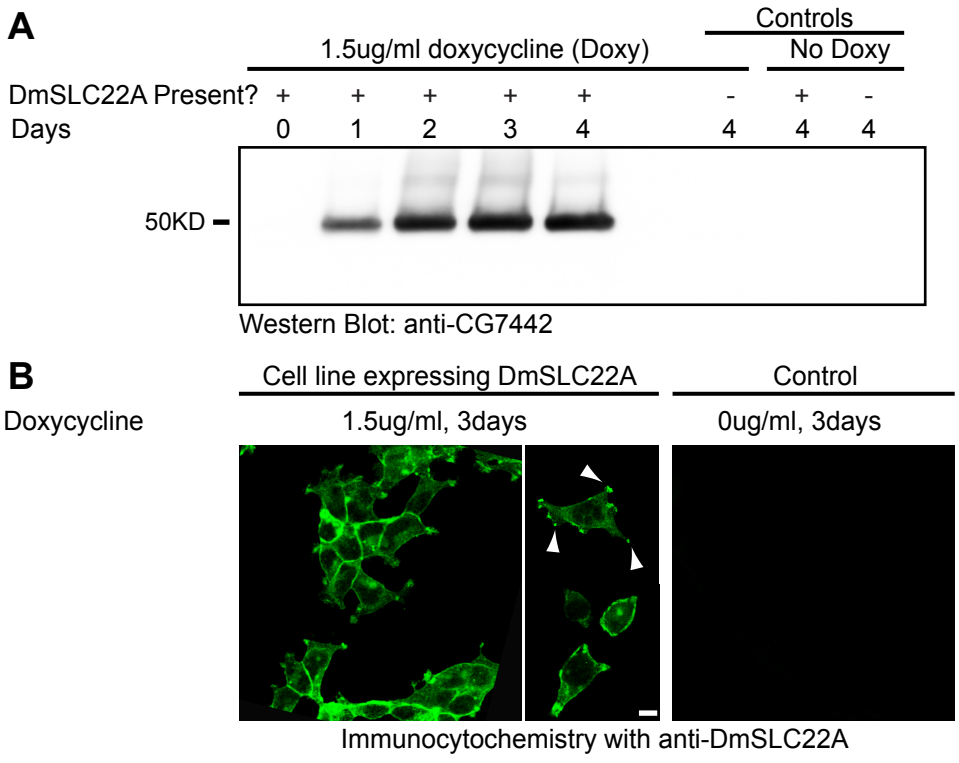
A
Controls
1.5ug/ml doxycycline (Doxy)
No Doxy
DmSLC22A Present? + + + + + - + -
Days 0 1 2 3 4 4 4 4
50KD
Western Blot: anti-CG7442
B
Cell line expressing DmSLC22A
Control
Doxycycline
1.5ug/ml, 3days
0ug/ml, 3days
Immunocytochemistry with anti-DmSLC22A

Figure S6, Related to Figure 6. Doxycycline-induced expression of DmSLC22A in a HEK293 stable cell line. (A) Western blotting of induced DmSLC22A expression with 1.5 µg/ml doxycycline in the HEK293-DmSLC22A stable cell line across four days. No signal was detected in cells without doxycycline or in HEK cells without the *DmSLC22A* construct. **(B)** The induced DmSLC22A in HEK293 cells was properly targeted to the plasma membrane, revealed by immunocytochemistry (green) and concentrated in focal adhesions (arrowheads). The two smaller images show higher magnifications of DmSLC22A expressing cells. No leaky expression was detected in the engineered cells without doxycycline induction (right panel). Scale bar = 10 µm.

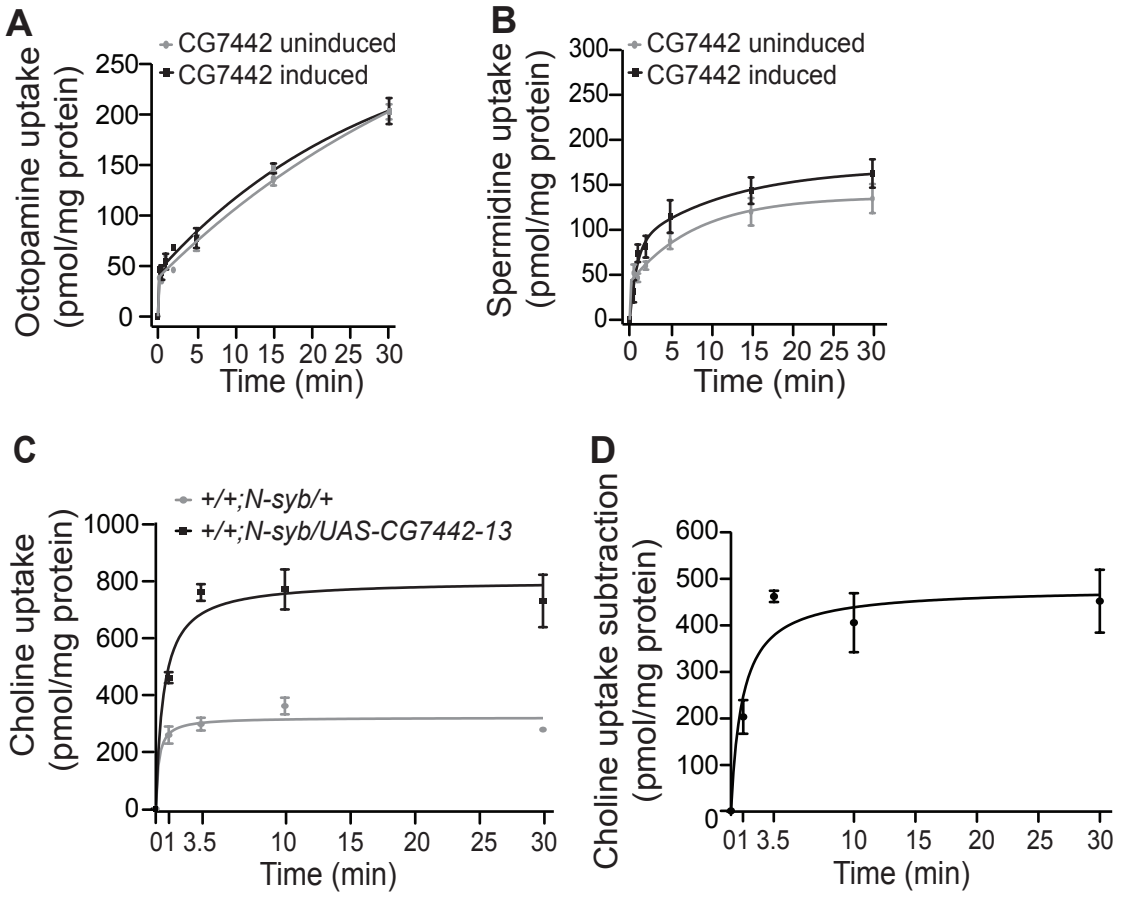
A
CG7442 uninduced
CG7442 induced
Octopamine uptake (pmol/mg protein)
Time (min)
B
CG7442 uninduced
CG7442 induced
Spermidine uptake (pmol/mg protein)
Time (min)
C
+/+;N-syb/+
+/+;N-syb/UAS-CG7442-13
Choline uptake (pmol/mg protein)
Time (min)
D
Choline uptake subtraction (pmol/mg protein)
Time (min)

Figure S7, Related to Figure 6. *In vitro* substrates identified using *a* stable HEK293 cell line and fly neurons overexpressing DmSLC22A. (A, B) DmSLC22A overexpression was induced by 1.5 µg/ml doxycycline for three days, while untreated cells were employed in parallel as control. Uptake of each compound in DmSLC22A expressing cells (black line) and un-induced cells (gray line) was plotted (pmol/mg total protein) at times across minutes. Two compounds were tested here, **(A)** octopamine and **(B)** spermidine. Both failed as effective substrates. **(C)** Choline uptake (pmol/mg protein) across 30m by control *Drosophila* brain neurons and those overexpressing DmSLC22A. Asymptotic uptake was reached within 5m under these conditions. **(D)** Difference plot of data in panel (C). Results are plotted as means ± SEM. All experiments were performed in triplicate for each of three biological samples.

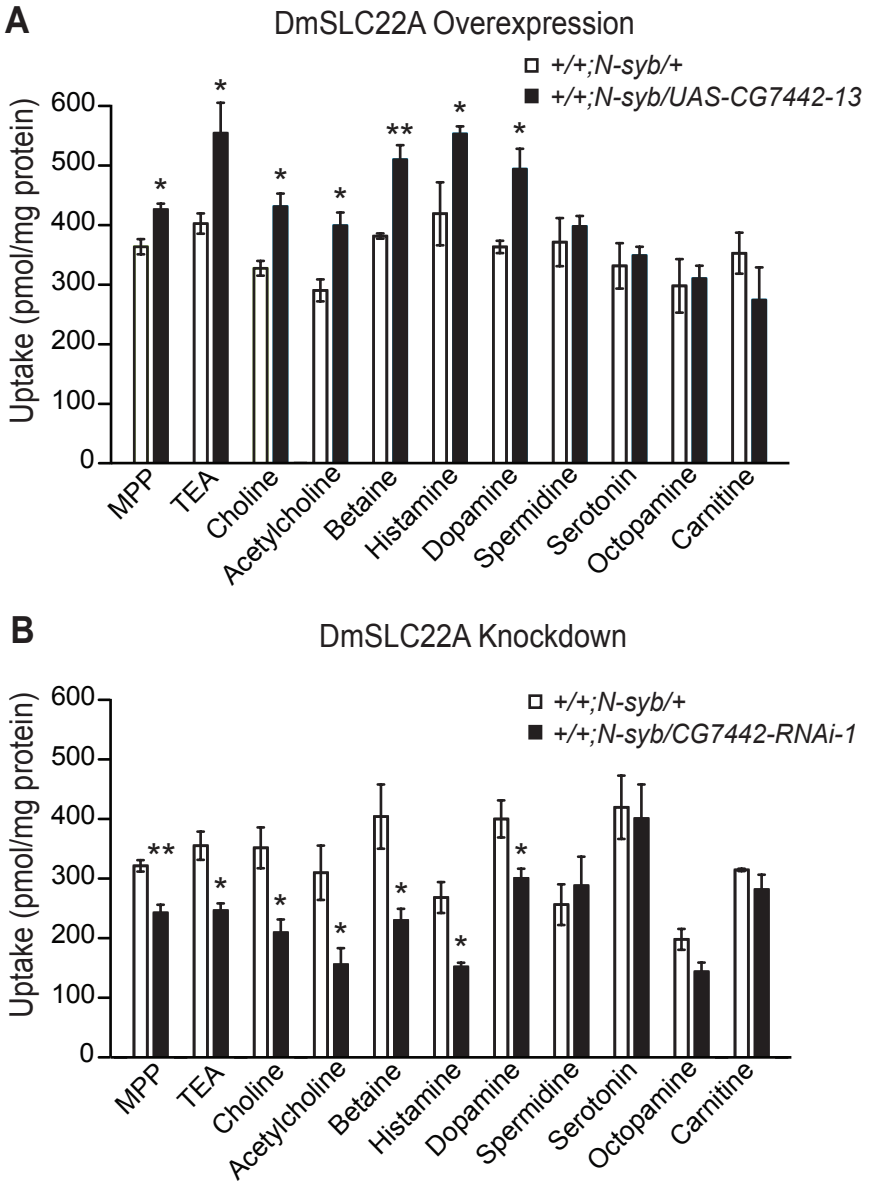
A
DmSLC22A Overexpression
+/+;N-syb/+
+/+;N-syb/UAS-CG7442-13
Uptake (pmol/mg protein)
0
100
200
300
400
500
600
MPP
TEA
Choline
Acetylcholine
Betaine
Histamine
Dopamine
Spermidine
Serotonin
Octopamine
Carnitine
B
DmSLC22A Knockdown
+/+;N-syb/+
+/+;N-syb/CG7442-RNAi-1
Uptake (pmol/mg protein)
0
100
200
300
400
500
600
MPP
TEA
Choline
Acetylcholine
Betaine
Histamine
Dopamine
Spermidine
Serotonin
Octopamine
Carnitine

Figure S8, Related to Figure 6. Transporter activity assayed using fly neurons with DmSLC22A overexpression or knockdown. Transport activity was assayed using adult brain neurons disassociated from control (*N-syb-gal4*>+), overexpressing (*N-syb-gal4>CG7442*), and knockdown flies (*N-syb-gal4>CG7442-RNAi).* Three technical replicates were performed for each substrate using three different biological samples. *Statistics:* Results are plotted as means ± SEM with * $P<0.05$, ** $P<0.01$.

Movie S1, Related to Figure 3. Super-resolution image of a slice of a portion of the MB calyx stained with anti-DmSLC22A (green) and anti-Brp^{nc82} (magenta). This movie shows the non-overlapping location between DmSLC22A in the MBn dendrites and the pre-synaptic boutons identified with Bruchpilot expression.

Table S1, Related to Figure 1, 2, and 5. Odor and shock avoidance

Genotype	Ben	Oct	Shock
Dicer2/+;238Y-gal4/+	0.80±0.02	0.72±0.07	0.69±0.05
CG7442-RNAi-1/dicer2;238Y-gal4/+	0.83±0.03	0.73±0.04	0.70±0.05
**Dicer2/+;238Y-gal4/+*	0.49±0.05	0.65±0.03	0.61±0.03
**CG7442-RNAi-1/dicer2;238Y-gal4/+*	0.53±0.06	0.66±0.05	0.57±0.07
Dicer2/+;R13F02-gal4/+	0.88±0.03	0.78±0.04	0.65±0.07
CG7442-RNAi-1/dicer2;R13F02-gal4/+	0.89±0.03	0.84±0.03	0.63±0.07
c772-gal4/+;dicer2/+	0.72±0.02	0.74±0.02	0.63±0.02
c772-gal4/CG7442-RNAi-1;dicer2/+	0.70±0.05	0.76±0.03	0.62±0.02
Dicer2/+;+/+;OK107-gal4/+	0.77±0.06	0.74±0.03	0.78±0.03
Dicer2/ CG7442-RNAi-1;+/+;OK107-gal4/+	0.83±0.03	0.80±0.04	0.82±0.04
c305a-gal4/+;dicer2/+	0.86±0.04	0.89±0.03	0.63±0.06
c305a-gal4/CG7442-RNAi-1;dicer2/+	0.83±0.03	0.90±0.02	0.64±0.05
Dicer2/+;R28H05-gal4/+	0.76±0.06	0.76±0.02	0.44±0.07
CG7442-RNAi-1/dicer2;R28H05-gal4/+	0.82±0.03	0.80±0.04	0.44±0.06
Dicer2/y;+/+;N-syb-gal4/+	0.79±0.01	0.82±0.03	0.62±0.03
Dicer2/y;CG7442-RNAi-1/+;N-syb-gal4/+	0.77±0.03	0.84±0.02	0.62±0.04
Dicer2/+;TH-gal4/+	0.82±0.04	0.78±0.04	0.65±0.07
CG7442-RNAi-1/dicer2;TH-gal4/+	0.82±0.03	0.71±0.04	0.59±0.04
+/+;238Y-gal4/+	0.66±0.05	0.42±0.05	0.59±0.06
+/+;238Y-gal4/UAS-CG7442-13	0.65±0.03	0.45±0.03	0.62±0.02
+/+;R13F02-gal4/+	0.52±0.05	0.50±0.07	0.69±0.03
+/+;R13F02-gal4/UAS-CG7442-13	0.47±0.08	0.44±0.04	0.69±0.05
Dicer2/+;238Y-gal4/+	0.67±0.03	0.76±0.03	0.56±0.03
Dicer2/+;238Y-gal4/ CG7442-RNAi-2	0.69±0.05	0.72±0.03	0.57±0.02
Dicer2/+;+/+;OK107-gal4/+	0.75±0.05	0.79±0.03	0.59±0.06
Dicer2/+;CG7442-RNAi-3/+;OK107-gal4/+	0.69±0.04	0.78±0.06	0.59±0.04
Dicer2/+;238Y-gal4/+	0.42±0.05	0.73±0.07	0.70±0.04
RNAi-CG7442/dicer2;238Y-gal4/UAS-CG7442	0.40±0.09	0.76±0.04	0.72±0.06

Odor and shock avoidance for genotypes used in this study. Avoidance of Ben was tested at 0.5%, Oct at 1.5%, and shock at 90V. Asterisks (*) identify reduced odor (10X dilution) and shock stimuli (25V). No significant differences were found for any of the genotypes tested compared to the relevant control (listed pairwise) after two-tail Student's t-test. Ben, Benzaldehyde. Oct, Octanol.

Table S2, Related to Figure 6 and S8. Km and Vmax values for DmSLC22A substrates

Substrates	HEK 293 cells			
	K_m (μM)	V_{max} (pmol/mg/min)	V_{max}/K_m	Efficiency*
Choline	0.7 ± 0.1	36.2 ± 6.8	51.7	70.9
Acetylcholine	2.7 ± 0.6	45.7 ± 7.9	17.2	23.6
Betaine	10.8 ± 2.3	141.4 ± 28.3	13.1	18.0
Dopamine	12.6 ± 0.4	177.6 ± 12.0	14.1	19.4
Histamine	13.1 ± 2.1	217.7 ± 36.2	16.6	22.7
L-carnitine	28.8 ± 7.3	596.2 ± 69.2	20.7	28.4
Serotonin	64.9	480.5	7.4	10.2
MPP	40.9	146.1	3.6	4.9
TEA	28.9	2106.6	72.9	100.0

Substrates	*Drosophila* neurons			
	K_m (μM)	V_{max} (pmol/mg/min)	V_{max}/K_m	Efficiency*
Choline	1.1 ± 0.0	122.9 ± 62.4	107.8	100.0
Acetylcholine	6.1 ± 0.4	629.7 ± 299.9	103.1	95.6
Betaine	10.8 ± 2.2	397.6 ± 196.6	36.8	34.1
Dopamine	9.8 ± 0.3	417.1 ± 37.4	42.7	39.6
Histamine	11.9 ± 2.3	161.5 ± 65.7	13.5	12.6

Experiments using choline, acetylcholine, betaine, dopamine, histamine and L-carnitine were performed in triplicate for each of three biological samples. Experiments using serotonin, MPP and TEA were performed in triplicate with one biological sample. *relative to TEA or choline.

Supplemental Experimental Procedures

Fly Stocks and Genetics

Flies were raised on standard food at 25^{o}C unless indicated otherwise. The *gal4* lines used in this study, all carrying *UAS-dicer2*, include: *238y-gal4*, *R13F02-gal4*, *VT64246-gal4*, *MZ604-gal4*, *NP2492-gal4*, *GH146-gal4*, *TH-gal4*, *alrm-gal4, repo-gal4, NP2222-gal4* and *mz0709-gal4.* The latter four glial *gal4* lines were the generous gift of Marc Freeman. The *UAS* lines used in this study include: *UAS-CG7442*-RNAi-1 (KK106555), *UAS-CG7442*-RNAi-2 (GD8450), *UAS-CG7442*-RNAi-3 (BL35817), *UAS-CG7442*-13, and *UAS-CG7442*-10. *R13F02-LexA and LexAop-CG7442* lines were also employed. The open reading frame of DmSLC22a was used to fabricate the pUAST constructs *UAS-CG7442*-10 and -13.

Behavioral Tests

Two to four day-old flies were used for all behavioral experiments. Flies were collected ~24h prior to conditioning and transferred to the behavioral room 30m before training to adapt to training conditions (dim red light, 25^{o}C, 75% humidity). Standard aversive olfactory learning was used as described (Beck et al., 2000; Berry et al., 2012). For conditioning, flies were placed into a training tube and received the following stimuli: 30s of fresh air, 1m of odor A paired with 12 pulses of 90V electric shock (CS+), 30s of fresh air, 1m of odor B without electric shock (CS-), and finally 30s of air. Odor streams were produced by bubbling fresh air through 3-octanol (OCT) or benzaldehyde (BEN) dissolved in mineral oil. For 3m memory tests, conditioned flies were transferred immediately after conditioning to a T-maze allowing them to choose for 2m between arms carrying air streams of either the CS+ or CS- odors. For memory retention, flies were tapped back into food vials after training and tested at the times indicated. To avoid naive odor bias, two groups of flies were trained and tested simultaneously; the first trained using BEN as CS+ and OCT as CS-, and the second trained using OCT as CS+ and BEN as CS-. Each group (~60 flies) tested provided a half-performance index (PI): half-PI = [(number of flies in CS- arm) – (number in CS+ arm)/(total number in both arms)]. A final PI was calculated by averaging the two half PIs. Odors and shock avoidance were tested as described (Berry et al., 2012). The avoidance index was calculated as ([number of flies in the arm with fresh air)–(number of flies in the arm with odor)])/total number of flies in both arms. For shock avoidance, flies were allowed to choose between T-maze arms containing the electrified copper grid (90V) or non-electrified copper grid for 2m.

Memory acquisition curves were performed using the short training program: 30s fresh air, 10s of CS+ odor paired with one pulse of 90V electric shock (delivered 8s after odor onset), 30s of fresh air, 10s of CS-odor without electric shock, and 30s of air. Flies were immediately tested for memory performances after training using one or multiple cycles of the above training schedule (Beck et al., 2000).

For proactive interference experiments, flies were trained with the odor pair of MES/MCH and re-trained with the second order pair of OCT/BEN using the standard conditioning protocol described above. A test using OCT and BEN was performed

immediately after the second training session. For retroactive interference experiments, flies were trained with the odor pair of OCT/BEN and re-trained 1.5h after with the second order pair of MES/MCH. A test using OCT and BEN was performed 3h after the second training session.

Anesthesia-resistant memory was measured by introducing a cold shock between conditioning and the test at 1.5h after conditioning. The cold shock was produced by transferring flies to a precooled glass vial in ice water for 2m, and then tapped back to the food vial for a 3h memory test.

For dietary supplementation experiments, flies were starved for 16-18h and then raised on filter paper saturated with 5.0% sucrose with or without 1.0% DmSLC22A substrate precursor (choline chloride, L-dopa or histidine) overnight (Zhang et al., 2008). Flies were transferred to fresh food vials 15m prior to conditioning. Memory tests performed at 6h were used to avoid ceiling/floor effects for the DmSLC22A knockdown group.

Functional Imaging

Calcium responses to odor stimulation of flies were recorded as previously reported (Berry et al., 2012). Briefly, a small, square section of dorsal cuticle was removed from the head of a single fly, which was immobilized to the imaging chamber using myristic acid. Fresh saline (103 mM NaCl, 3 mM KCl, 5 mM HEPES, 1.5 mM $CaCl_2$, $MgCl_2$, 26 mM $NaHCO_3$, 1 mM NaH_2PO_4, 10 mM trehalose, 7 mM sucrose, and 10 mM glucose [pH 7.2]) was added to cover the whole brain to prevent desiccation and ensure the health of the fly. The GCaMP6.0f imaging was performed using a Leica TCS SP5 II laser-scanning confocal microscope with a 25X water-immersion objective. The MB calyx area was selected as the region of interest (ROI); frames were scanned with a 488nm laser and collected at the frequency of 2 frames/s in a 2 min recording session. GCaMP6.0f activity in the calyx in response to odor stimulation was transformed using custom algorithms previously described (Berry et al., 2012). The GCaMP6.0f intensity traces were normalized and plotted as the percentage fluorescence change ($\%\Delta F/F_0$), and the maximum GCaMP6.0f fluorescence change across each trace was calculated for each genotype.

Molecular Biology

Messenger RNA expression in control and DmSLC22A overexpression and knockdown flies was measured by qRT-PCR. First-strand cDNA was transcribed (SuperScript® III First-Strand Synthesis System, Invitrogen) from total RNA isolated from fly heads (TRIzol, Invitrogen; RNeasy Mini Kit, QIAGEN) according to manufacturers' protocols. Real-time PCR analysis was performed using SYBR green (Quantitect, QIAGEN). The expression data were collected using ABI Prism 7900HT (Applied Biosystems) with normalization to glyceraldehyde 3-phosphate dehydrogenase (GAPDH). All final PCR products were sequenced to verify the specificity of amplification. The primers used for cDNA amplification were: For CG7442 (forward) 5'-TGCTCACGCTGTTCTTTCCA-3', (reverse) 5'-CGATTGCTTCTTGACGCCTAT-3'. For GAPDH (forward) 5'-CCCATAGAAAGCGCTCAAAA-3', (reverse) 5'-CCAATCTTCGACATGGTTAACTT-3'.

Bioinformatics of protein sequence similarity were performed using BLAST (http://blast.ncbi.nlm.nih.gov/Blast.cgi). Clustal X2.0 was used for multiple protein sequence alignment. Transmembrane domains (TM) were predicted by the Simple Modular Architecture Research Tool (http://smart.embl-heidelberg.de/) and the NJ phylogenic tree was built based on protein sequences of DmSLC22A and all human SLC22A family members using MEGA6.0.

Antibody Generation, Western Blotting and Immunohistochemistry

A hydrophilic region of CG7442 was cloned into the expression vector pGEX-4T-1 and GST-fusion protein expression was induced in *E.coli* BL21 (Invitrogen) with 1 mM IPTG. The expressed fusion protein was purified using the Glutathione Sepharose High Performance System (GE healthcare) according to manufacturer's protocols and analyzed by SDS-PAGE electrophoresis. Polyclonal antisera was produced in *guinea pig* against the fusion protein by Pocono Rabbit Farm & Laboratory. Antibodies against the GST sequences were cleared from sera by affinity chromatography with column matrix coupled to GST. Antibodies specifically directed to DmSLC22A were further purified using affinity chromatography to column matrix coupled to the fusion protein. A monoclonal antibody (#435) was raised in the mouse against the sequence DKLQQSSESRFP in the large intracellular loop connecting TM6 and TM7 by Abmart.

For western blotting, fly heads were homogenized in RIPA buffer (Cell Signaling Tech.) with added protease inhibitor (Roche). Lysates equivalent to 12 fly heads were mixed with Laemmli Sample Buffer (Bio-Rad) and kept at room temperature for at least 20m followed by standard SDS-PAGE. Primary antibodies used include: polyclonal anti-CG7442 (*guinea pig* 1:2,000) and anti-GAPDH (rabbit 1:1,000, GeneTex Cat# GTX100118, RRID: AB_1080976). HRP-conjugated secondary antibodies were used at a 1:10,000 dilution. Chemiluminescence signals were detected using the ECL Blotting Kit (BioExpress) and the band intensity quantified with ImageJ.

For immunochemistry, dissected fly brains were fixed for 30m at room temperature in 4% paraformaldehyde followed by a 5m re-fixation with 80% acetone at -20°C and processed as described (Mao and Davis, 2009). Primary antibodies used included: polyclonal anti-CG7442 (*guinea pig* 1:100), monoclonal anti-CG7442 (mouse 1:100), anti-Brp^{nc82} (mouse 1:50, DSHB Cat# nc82, RRID: AB_528108), and anti-GFP (rabbit 1:1000, Invitrogen Cat# A6455, RRID: AB_221570). Secondary antibodies included Alexa 488, 546, 633 or 647 (1:400; Molecular Probes). Confocal images were collected on Leica TCS SP5 II and super resolution images were collected on Zeiss ELYRA S1. Fluorescence images were processed using ImageJ and Adobe Photoshop.

Transporter Assays

HEK293 cells were cultured in complete DMEM medium supplemented with 10% FBS, 100 units/ml Strep/Pen at 37°C, and 5% CO_2. The open reading frame of CG7442 cDNA was cloned into the expression vector pcDNA™5/FRT/TO (Invitrogen) and co-transfected with pOG44 at a ratio of 1:9 (w/w) into Flp-In™T-REx™ 293 cells using Lipofectamine™ 2000 (Invitrogen). Stable transformants were selected with 200 µg/ml HygromycinB, and single-cell colonies were isolated from limited dilution and tested for

Zeocin™ sensitivity (100 µg/ml, Invitrogen). The presence of the CG7442 open reading frame was tested by PCR. Transient protein expression was induced by doxycycline (1.5 µg/ml, Sigma) and verified by western blotting and immunocytochemistry.

The radiolabeled compounds [^{14}C] TEA^+ (tetraethylammonium), [^{3}H] MPP^+ (Methyl-4-phenylpyridinium), [^{14}C] $choline^+$, [^{3}H] $acetylcholine^+$, [^{3}H] $octopamine^+$, [^{3}H] $L\text{-}carnitine^+$, [^{3}H] $betaine^+$, [^{3}H] $dopamine^+$, [^{3}H] $histamine^{2+}$, [^{14}C] $spermidine^{3+}$, and [^{14}C] $serotonin^+$ were purchased from American Radiolabeled Chemicals and PerkinElmer. Recombinant Flp-DmSLC22A HEK cells were seeded at a density of $0.5X10^5$ cell/well on 12-well plates. After cells attachment, 1.5 µg/ml doxycycline was added for experimental wells. Cells were incubated for 48-72h to reach ~80-90% confluence. Transport activity was assayed at 37°C in Waymouth's buffer (WB: 135 mM NaCl, 13 mM HEPES, 2.5 mM $CaCl_2$, 1.2 mM $MgCl_2$, 0.8 mM MgSO4, 5 mM KCl, and 28 mM D-glucose) containing radiolabeled compounds as described in Belzer et al, 2013. Transport activity was terminated by washing the cells three times with ice-cold WB buffer. The cells were then solubilized in 1N NaOH with 1.5% SDS and neutralized with 1N HCl. The radioactivity was measured using liquid scintillation spectroscopy and protein concentration was measured using the Bio-Rad Protein Assay (Bio-Rad Laboratories). For all data, the uptake of substrate was normalized to protein content and represented as pmol/mg protein. For the kinetic experiments, the compound of interest was incubated at 7 different concentrations with cells and the initial transport velocity was measured at either 30 or 60s. Kinetic parameters (Km and Vmax) were calculated using Lineweaver–Burk plots. The transport activity of control cells was subtracted from the experimental groups in order to measure DmSLC22A-specific transporter activity. All experiments were performed in triplicate and repeated at least three times.

Adult flies brains were quickly dissected in cold Schneider's medium and brain neurons were disassociated as described (Egger et al., 2013). Transport assays were performed as described for HEK cells with minor modifications. Rinaldini solution (R-solution, 8 mg/ml NaCl, 0.2 mg/ml KCl, 0.05 mg/ml $NaH_2PO_4\text{-}H_2O$, 1 mg/ml $NaHCO_3$, 1 mg/ml glucose and 1% Pen-strep) was used for transport experiments with fly neuron suspensions. Cells were pelleted by centrifugation at 1600rpm, 5m after incubation with radiolabeled compounds and between washing steps. Siliconized tips and Eppendorf tubes were used to reduce cell lose. All experiments were performed in triplicate and repeated at least three times.

Statistical Analyses

Prism 5.0 was used for statistical analyses. Two-tailed t-tests were used to compare two groups. One-way ANOVA with a Tukey *post hoc* comparison between the relevant groups was used for data presented in Figure 5C-E. Two-way ANOVA was performed when both genotype and time were variables parameters. Confidence levels were set at $p \leq 0.05$, $^*P<0.05$, $^{**}P<0.01$, $^{***}P<0.001$.

Supplemental References

Belzer, M., Morales, M., Jagadish, B., Mash, E.A., and Wright, S.H. (2013). Substrate-dependent ligand inhibition of the human organic cation transporter OCT2. J. Pharm. Exp. Ther. *346*, 300–310.

Berry, J.A., Cervantes-Sandoval, I., Chakraborty, M., and Davis, R.L. (2015). Sleep facilitates memory by blocking dopamine neuron mediated forgetting. Cell *161*, 1656-1667.

Egger, B., van Giesen, L., Moraru, M., and Sprecher, S.G. (2013). In vitro imaging of primary neural cell culture from *Drosophila*. Nat. Protoc. *8*, 958-965.

Mao, Z., and Davis, R.L. (2009). Eight different types of dopaminergic neurons innervate the *Drosophila* mushroom body neuropil: anatomical and physiological heterogeneity. Front. Neural Circuit. *3*, 5-17.

Zhang, S., Yin, Y., Lu, H., and Guo, A. (2008). Increased dopaminergic signaling impairs aversive olfactory memory retention in *Drosophila*. Biochem. Biophys. Res. Comm. *370*, 82-86.